



**HAL**  
open science

# **Anisole laser induced fluorescence (LIF) for imaging local heterogeneities in temperature in a rapid combustion machine**

K.H. Tran, M. Kühni, C. Morin, P. Guibert

► **To cite this version:**

K.H. Tran, M. Kühni, C. Morin, P. Guibert. Anisole laser induced fluorescence (LIF) for imaging local heterogeneities in temperature in a rapid combustion machine. European Combustion Meeting ECM 2011, ECM, Jun 2011, Cardiff, United Kingdom. <hal-04459348>

**HAL Id: hal-04459348**

**<https://hal.science/hal-04459348v1>**

Submitted on 15 Feb 2024

**HAL** is a multi-disciplinary open access archive for the deposit and dissemination of scientific research documents, whether they are published or not. The documents may come from teaching and research institutions in France or abroad, or from public or private research centers.

L'archive ouverte pluridisciplinaire **HAL**, est destinée au dépôt et à la diffusion de documents scientifiques de niveau recherche, publiés ou non, émanant des établissements d'enseignement et de recherche français ou étrangers, des laboratoires publics ou privés.



HAL Authorization

# Anisole laser induced fluorescence (LIF) for imaging local heterogeneities in temperature in a rapid combustion machine

K.H. Tran\*, M. Kühni, C. Morin, P. Guibert

Institut Jean Le Rond d'Alembert - CNRS UMR 7190

Université Pierre et Marie Curie (Paris 6)

2, place de la Gare de Ceinture 78210 Saint-Cyr-l'Ecole France

## Abstract

The aim of the study is to characterize the local temperature heterogeneities for HCCI combustion mode in a rapid compression machine (RCM), where temperature and pressure vary simultaneously. The technique of Laser Induced Fluorescence (LIF) is used with one excitation wavelength and two integration spectral bands. Fluorescence signal depends on several parameters such as temperature, pressure, tracer concentration, bath gas and laser energy. Firstly it is necessary to perform a parametric analysis and a calibration in a high pressure-high temperature (HP-HT) vessel, before investigation in controlled conditions such as in a RCM.

## Introduction

A precise knowledge of thermodynamic conditions such as the concentration, the temperature and the pressure is essential for present combustion and pollutant formation in IC engine. The technique of laser induced fluorescence (LIF) was developed for the temperature measurement in controlled conditions such as in a Rapid Compression Machine (RCM), engine, shock tube or heated flow cell [1-3]. Most of tracers commonly used in the literature are, aromatics, polycyclic aromatic hydrocarbons (PAHs) and ketones which have a high fluorescence quantum yield (toluene  $\phi_f = 0.17$ , benzene  $\phi_f = 0.22$ ) [4].

In a global and macroscopic balance formulation, the fluorescence signal depends for weak excitation on thermodynamics parameters according to the following equation:

$$S_f = \frac{E}{hc/\lambda} \eta_{opt} dV_c \left[ \frac{X P}{kT} \right] \sigma(\lambda, T) \Phi(\lambda, T, P, \sum_i X_i) \quad (1)$$

with E the laser fluence, ( $hc/\lambda$ ) the energy of a photon at the excitation wavelength,  $\eta_{opt}$  the overall efficiency of the collection optics,  $dV_c$  the collection volume,  $\sigma$  the molecular absorption cross section of the tracer,  $\Phi$  the fluorescence quantum yield, X the mole fraction, P the total pressure, k the Boltzmann constant and T the temperature.

Different LIF techniques exist to measure the temperature based on Eq. (1), the selection of one of them is dictated by thermodynamic quantities to study, the selected tracer, thus the experimental conditions.

The first one is the single color detection technique used for homogeneously seeded flows. This technique is restrictive as it applies in constant total pressure conditions, with homogeneous concentration distribution at constant volume.

Experimental conditions have to be set such as laser intensity, excitation wavelength, optical yield and volume. Thus the fluorescence signal is proportional to the tracer absorption cross section and the fluorescence quantum yield. The fluorescence signal evolves in  $1/T$  :

$$S_f \propto \frac{1}{T} \sigma(\lambda, T) \phi(\lambda, T, P) \quad (2)$$

The second technique is the single excitation two-color detection technique, it enables to measure fluorescence signal in inhomogeneously seeded flow. In fact, we take away from homogeneously tracer concentration condition thanks to the two integration bands ratio. The detected fluorescence signal ratio of spectral bands  $\Delta\lambda_1$  and  $\Delta\lambda_2$  is presented below:

$$\frac{S_f^{\Delta\lambda_1}(x, y, T, P)}{S_f^{\Delta\lambda_2}(x, y, T, P)} \propto \frac{\phi^{\Delta\lambda_1}(T(x, y), P)}{\phi^{\Delta\lambda_2}(T(x, y), P)} = f(T(x, y)) \quad (3)$$

The fluorescence signal ratio is proportional to the temperature.

The third technique is the dual-excitation wavelength technique. It also enables to measure fluorescence signal in inhomogeneously seeded flow. This technique is applied in case where the tracer partial pressure varies and the tracer concentration is inhomogeneous. The fluorescence signal ratio from two excitation wavelengths  $\lambda_1$  and  $\lambda_2$  gives:

$$\frac{S_{f, \lambda_1} E_{\lambda_1}}{S_{f, \lambda_2} E_{\lambda_2}} \propto \frac{\sigma(\lambda_2, T) \phi(\lambda_2, T, P)}{\sigma(\lambda_1, T) \phi(\lambda_1, T, P)} \quad (4)$$

This last technique enables to obtain a better signal to noise ratio than the second technique, whereas it requires an important experimental set up and a high cost because it involves two lasers with pulses slightly delayed to ensure separate detection of the two fluorescence signals in the same wavelength band.

In our study, the second technique is selected, taking account on experimental conditions noted

\* Corresponding author: kxanh-hung.tran@upmc.fr  
Proceedings of the European Combustion Meeting 2011

later, and satisfactory fluorescence signal compared to the first technique.

The single excitation two-color detection technique was used by Luong et al. [3] with the excitation wavelength of 248 nm and toluene in air over a temperature range of 300-675 K in shock tube and heated flow-cell for in-cylinder temperature distribution measurements. Kaiser et al. [5] also used this technique with the excitation wavelength of 266 nm and naphthalene as tracer in nitrogen and oxygen over a temperature range of 400-928 K at 0.1 MPa for equivalent ratio and temperature imaging.

### Specific objectives

The single-excitation two-colour detection technique for the temperature measurement depends on pressure and temperature which have an influence on the variations of the absorption cross section and the fluorescence quantum yield. Preliminary it is necessary to investigate a fluorescence signal calibration in a set up where thermodynamic conditions are perfectly known. So a prior study has been realised in a high pressure and high temperature (HP-HT) cell over a large range of temperature (473-773 K) and pressure (0.2-4 MPa) to determine the selection of the tracer, the optimal concentration, the excitation wavelength and the laser intensity in order to obtain a satisfactory fluorescence signal with different sensibilities according to the temperature and the integration bands selected.

### Experimental set-up

The fluorescence signal calibration of tracer is realised in a HP-HT cell, as shown in Fig.1 and described in Ref [6]. The inside volume is  $7.6969 \times 10^{-4} \text{ m}^3$ , heated and maintained at constant temperature by eight electrical resistance (230 W each). A system composed of three thermocouples inside the cell enables to regulate it and ensures the cell temperature homogeneously. The liquid fuel/tracer blend is vaporized by reaching the boiling point and the saturate vapour pressure thanks to vacuum pump in the inside volume. An admission circuit composed of pressure sensors and flood gates enables to up the cell under pressure with different bath gases. The optical system is composed of a frequency-quadrupled and pulsed Nd:Yag laser (266 nm, 90 mJ/pulse at 10 Hz). The pulse width fluctuation is 3-4 nm with an energetic stability of  $\pm 8 \%$ . The laser beam crosses over the centre of the cell and it is recovered by a beam trap and a fluxmeter that enables to know the temporal laser fluctuations and the laser intensity. The fluorescence signal is collected at  $90^\circ$  from the incident beam by a high sensitivity spectrometer supplied with an UV lens (motorized slit, three diffracting gratings of 150, 600 and 1200 grooves per mm, integration time of 150  $\mu\text{s}$ ), and an ICCD camera supplied with an UV lens. The filters are placed at front of measurement devices.

Several tracers were tested in order to select the more appropriate. Fluorescence spectra were measured for polycyclic aromatic hydrocarbons (fluoranthene  $\text{C}_{16}\text{H}_{10}$ ), aromatics (toluene  $\text{C}_7\text{H}_8$ , anisole  $\text{C}_6\text{H}_5\text{OCH}_3$ ), ketones (3-pentanone  $\text{C}_5\text{H}_{10}\text{O}$ , acetone  $\text{C}_3\text{H}_6\text{O}$ ) at 573 K and 0.2 MPa, for the excitation wavelength of 266 nm in nitrogen.

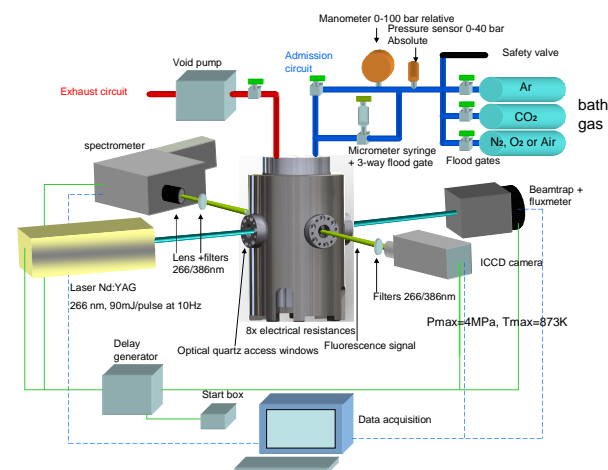


Figure 1: High pressure and high temperature device with optical system

These different tracers present low fluorescence signal in the explored experimental conditions, except anisole. This tracer is then selected for its satisfactory spectroscopy proprieties [7] and its physical proprieties close to these of isooctane ( $\text{C}_8\text{H}_{18}$ ), the traced fuel. The anisole is a methyl oxide-ether of phenol (cf. Fig. 2), it presents under liquid form. Anisole is a very volatile compound (100% at 294 K), its saturate vapour pressure is 0.0013 MPa at 315 K and its boiling point is equal to 429 K [8] that enables a good vaporization in our experimental conditions.

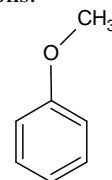


Figure 2: Anisole chemical structure

The HP-HT cell experiments are realised in different bath gases (nitrogen, argon, carbon dioxide and air), for a pressure range of 0.2-4 MPa and temperature range of 473-773 K. For given experimental thermodynamics conditions, the fluorescence signals are averaged from 900 emissions spectra. Every experiment is reproduced three times. The normal standard deviations are included between 1.5-15% for the different bath gases.

## Results and discussion

### Anisole absorption and fluorescence

For different LIF techniques, the absorption cross section is taken into account to calculate the

fluorescence signal which varies with the temperature and the excitation wavelength. At a constant excitation wavelength, the absorption cross section  $\sigma$  depends only on the temperature. It is deduced from Lambert-Beer's law:

$$\sigma(\lambda) = \frac{\ln [I_0(\lambda) / I(\lambda)]}{l * C} \quad (5)$$

with  $I_0$  the incident intensity,  $I$  the transmitted intensity,  $l$  the path length and  $C$  the anisole concentration.

As presented in Fig. 3, the absorption spectrum of anisole is located between 240-290 nm, as underlined in Ref [9] too. The absorption spectra comparison shows a maximum difference of absorption cross sections of 12% for different temperatures at 266 nm. It will be then necessary to normalize the fluorescence signal to the absorption cross section  $\sigma$  corresponding to a given temperature for the used excitation wavelength of 266 nm.

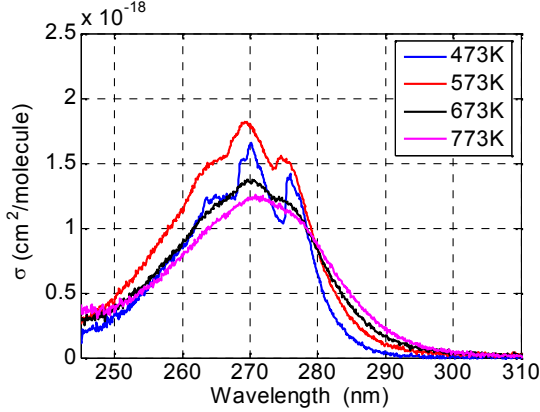


Figure 3: Absorption cross section of anisole for different temperatures in nitrogen at 0.2 MPa

The anisole fluorescence spectrum in isooctane is included between 270-400 nm, the peak is centred at 295 nm (cf. Fig.4 and Ref.[10-11]). This figure shows that fluorescence spectrum strongly decreases with increasing of the temperature, which underlines the interest of anisole as tracer for the measurement of temperature by LIF.

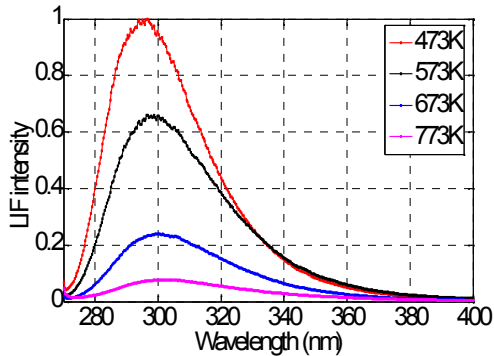


Figure 4: Normalized fluorescence spectra of anisole for different temperatures and a pressure of 0.8 MPa in nitrogen ( $\lambda_{exc} = 266$  nm). The fluorescence spectrum is normalized to the maximum value recorded at 473 K

As pictured in Fig. 5, the fluorescence signal evolution versus molecular density is represented for 2% anisole/isooctane blend. This concentration is selected to stay in the linear regime. The signal increases up to reach a saturation level which corresponds to  $1.4 \times 10^{12}$  molecule /  $cm^3$  at 473 K and  $2.15 \times 10^{12}$  molecule /  $cm^3$  for 773 K. After these respective maxima, the fluorescence signal decreases due to two quenching phenomena, the reabsorption and the auto-quenching (collision with anisole molecules in the ground state).

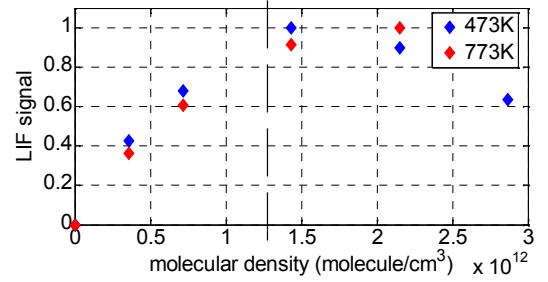


Figure 5: Evolution of normalized anisole fluorescence signal versus molecular density in nitrogen at 0.2 MPa, 473 K and 773 K for the excitation wavelength of 266 nm. The signal is normalized to the reference value obtained for the highest fluorescence signal. Dash line represents the experimental molecular density value.

Therefore to avoid these quenching phenomena, the experimental molecular density is fixed at  $1.29 \times 10^{12}$  molecule /  $cm^3$  (cf. Fig. 5). Similarly, all experiments are investigated in the linear fluorescence regime, with a laser energy laser fixed at 90 mJ/pulse.

### Pressure and temperature dependences of the anisole fluorescence signal

The anisole fluorescence signal depends on thermodynamics parameters such as temperature and pressure, as seen in Eq. (1). Therefore it is necessary to study independently the pressure influence at fixed temperature and the temperature influence at fixed pressure, to build a cartographic of signal intensity in function of pressure and temperature. When normalized to the molecular density, the fluorescence signal noted  $S_f^*$  is proportional to the fluorescence quantum yield  $\phi$  at fixed temperature and wavelength, as expressed in Eq. (6).

$$\frac{S_f^*(P)}{S_f^*(P_{ref})} \propto \left[ \frac{\phi(\lambda, T, P)}{\phi(\lambda, T, P_{ref})} \right] \quad (6)$$

The fluorescence signal decreases with the pressure as presented in Fig. 6. Indeed, it decreases by factor 2.5 (a decrease by a factor larger than two for 1,2,4-trimethylbenzene, [12]) when the pressure increases from 0.2 to 4 MPa. This decrease with the pressure depends on the temperature, whereas, it seems to have a low influence from 673 K. This

important decrease could be due to high collision rate leading to more non-radiative collisional deexcitation. It is noted that, for the ketones, the fluorescence signal increases with pressure [2], a similar evolution is observed for PAHs (naphthalene [13] and fluoranthene [6]).

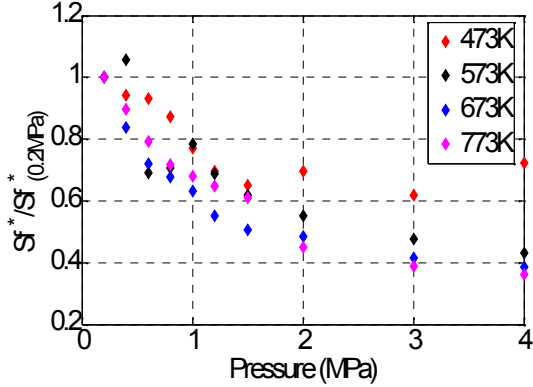


Figure 6: Influence of pressure on anisole fluorescence in nitrogen for different temperatures at 266 nm. The signal  $S_f^*$  is normalized to the molecular density and the reference value at 0.2 MPa.

It is necessary to take into account of the anisole absorption cross section to see the influence of temperature on the fluorescence quantum yield. Therefore the fluorescence signal  $S_f^*$  is normalized to the corresponding cross section value for a given temperature and excitation wavelength and is noted  $S_f^{**}$ , as presented in Eq. (7):

$$\frac{S_f^{**}(T)}{S_f^{**}(T_{ref})} \propto \left[ \frac{\phi(\lambda, T, P)}{\phi(\lambda, T_{ref}, P)} \right] \quad (7)$$

The anisole fluorescence quantum yield decreases with increasing temperature between 473-773 K, as observed in Fig.7. The sensitivity of the fluorescence signal is stronger to the temperature than the pressure. In fact, the fluorescence signal decreases with a factor of 5 for the explored temperature range. This fluorescence decrease is explained by the radiative mechanisms of intersystem crossing more efficient when the excited levels are energetic. A similar trends are observed in the literature for others tracers as acetone [2], 3-pentanone [1], for which the fluorescence quantum yield decreases with increasing temperature. As presented in Fig. 7, the fluorescence quantum yield decreases significantly, with a more marked decrease at high pressure. At 0.2 MPa, the fluorescence quantum yield decreases exponentially by one order of magnitude within the studied temperature range, the single exponential fit is given by:

$$\frac{\Phi(T)}{\Phi(473K)} \Big|_{266nm} = 16.299 \exp(-0.0057T) \quad (8)$$

With  $R^2 = 0.9674$

In comparison, Kühni et al. [6] have obtained the following exponential fit for the fluoranthene fluorescence quantum yield valid for 0.1 MPa nitrogen bath gas and 473-873 K:

$$\frac{\Phi(T)}{\Phi(473K)} \Big|_{266nm} = 71.42 \exp(-0.0095T) \quad (9)$$

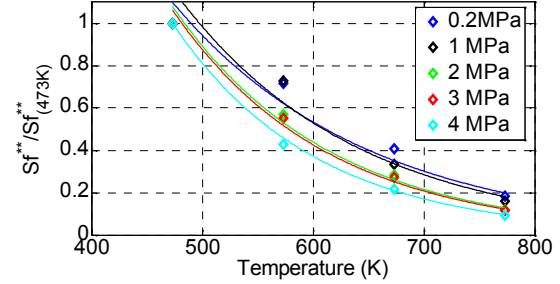


Figure 7: Influence of temperature on anisole fluorescence in nitrogen for several pressures. The signal is normalized to the molecular density, the absorption cross section and the reference value obtained at the temperature of 473K.

For imaging temperature by fluorescence, it is interesting to normalize the signal to the molar fraction and the absorption cross section for a given temperature. The fluorescence signal noted  $S_f^{++}$  depends then on the inverse of the temperature and can be used to convert the fluorescence signal into temperature from the dual-colour detection and one excitation wavelength technique for the temperature measurement:

$$\frac{S_f^{++}(T)}{S_f^{++}(T_{ref})} \propto \left[ \frac{T_{ref}}{T} \right] \cdot \left[ \frac{\Phi(\lambda, T, P)}{\Phi(\lambda, T_{ref}, P)} \right] \quad (10)$$

As pictured in Fig. 8, the fluorescence quantum yield decreases significantly in our temperature range, this evolution is similar for all the studied pressure.

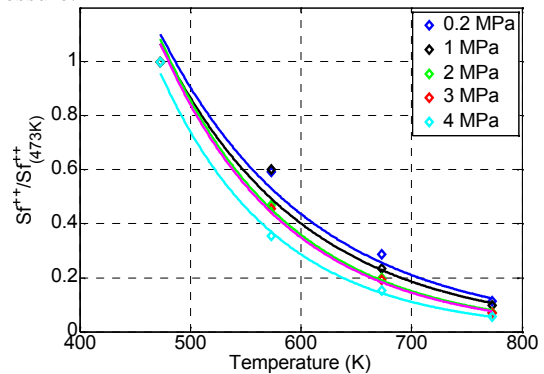


Figure.8: Influence of temperature on anisole fluorescence excited at 266 nm in nitrogen for different pressures. The signal  $S_f^{++}$  is normalized to the molar fraction, the absorption cross section and the reference value at 473 K.

The fluorescence decrease evolves as an exponential. For 0.2 MPa, within the studied temperature range, the exponential fit is written as:

$$\left. \frac{S_f^{++}(T)}{S_f^{++}(473K)} \right|_{266nm} = 34.828 \exp(-0.0073T)$$

With  $R^2 = 0.9843$  (11)

### Influence of the ambient gas

The influence of gas on anisole fluorescence is observed for nitrogen, carbon dioxide and argon. The evolution of the fluorescence signal versus pressure is similar for nitrogen and carbon dioxide, whereas for argon, the fluorescence signal decreases lower than in the two other gases, as shown in Fig. 9.

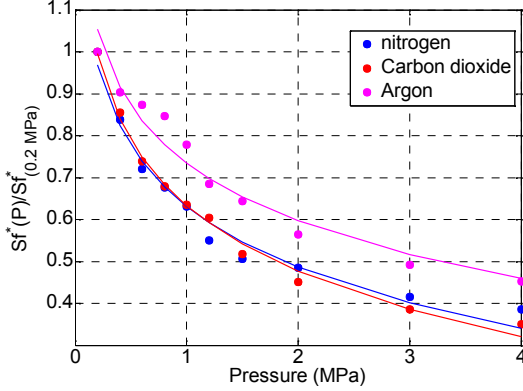


Figure 9: Influence of pressure on anisole fluorescence for different gases at 266 nm. The signal  $S_f^*$  is normalized to the molecular density and the reference value at 0.2 MPa.

### Implication for temperature measurement by the single-excitation two-color detection technique

From the previous results where the influence of pressure and temperature are characterized, temperature can be inferred from the ratio of measured fluorescence signals for two integration bands at the excitation wavelength of 266 nm. As pictured in Fig. 10, this ratio is a single function of temperature. For the studied pressures, the ratio of fluorescence signal shows a satisfactory sensitivity versus temperature.

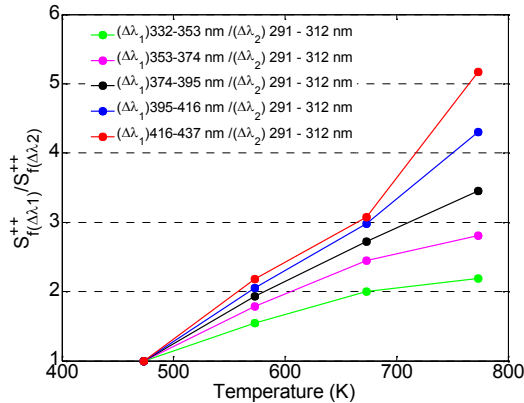


Figure 10: Evolution of the fluorescence signal ratio versus temperature in nitrogen at 1.2 MPa for the excitation wavelength of 266 nm.

Different integration bands were tested to optimize the ratio value. We have to take into account on the signal/noise ratio, concerning the integration band  $\Delta\lambda_2$  located at the fluorescence spectral queue. In fact, we take care to select only  $\Delta\lambda_2$  which present a signal/noise ratio with a factor of 2 or more at 773 K, as shown in Fig. 11. Integration bands selected are then  $\Delta\lambda_1 = 291-312$  nm and  $\Delta\lambda_2 = 374-395$  nm. The band integration  $\Delta\lambda_1$  corresponds to the central eak of the fluorescence spectrum. For the studied temperature range, the ratio value reaches 3.45, the ratio of fluorescence signal increases of 70% in nitrogen. The signal/noise ratio for  $\Delta\lambda_1$  and  $\Delta\lambda_2$  are equal respectively to 51.6 and 2.9.

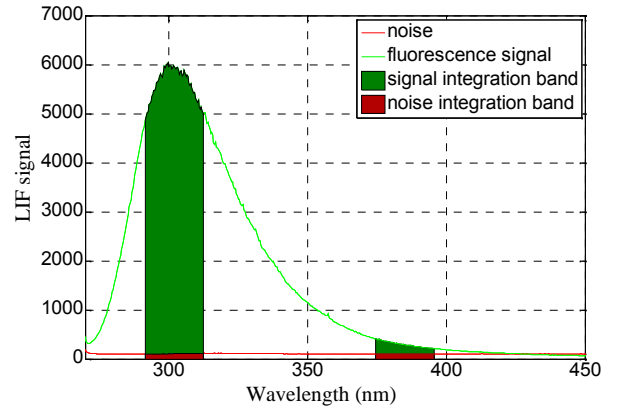


Figure 11: Anisole fluorescence and noise spectra with integration bands respectively located at  $\Delta\lambda_1 = 291-312$  nm and  $\Delta\lambda_2 = 374-395$  nm, for 1.2 MPa and 773 K in nitrogen.

Experimental fluorescence signal ratios plotted in Fig.12 decrease in our temperature range for different pressures in nitrogen. The fluorescence decreasing evolves as an exponential function.

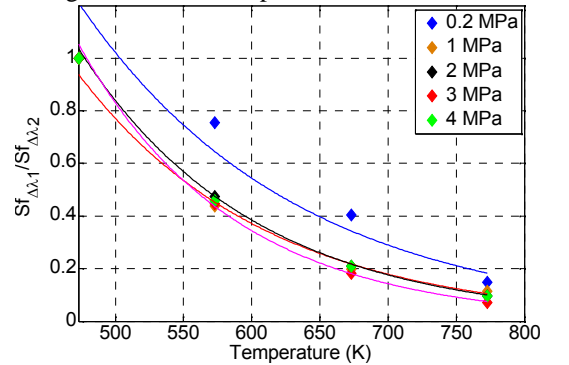


Figure.12: Evolution of the experimental fluorescence signal ratio versus temperature for different pressures in nitrogen, with  $\Delta\lambda_1 = 291-312$  nm and  $\Delta\lambda_2 = 374-395$  nm.

For a pressure of 3 MPa, the comparison between the calculating and experimental fitting gives a good agreement, as seen below.

Calculation fitting from the fluorescence signal

$$\frac{S_f(T)}{S_f(473K)} \Big|_{266nm} = 68.483 \exp(-0.0088T)$$

With  $R^2 = 0.9969$  (12)

Experimental fitting from the filtered signal

$$\frac{S_f(T)}{S_f(473K)} \Big|_{266nm} = 67.648 \exp(-0.0088T)$$

With  $R^2 = 0.9997$  (13)

## Conclusion

This study has investigated the influence of pressure, temperature and gas composition on anisole fluorescence in high-pressure and high-temperature device for the excitation wavelength of 266 nm. The aim of this parametric study is to calibrate the single-excitation two color detection technique for heterogeneity temperature measurements in a RCM using anisole as a new molecule tracer. This LIF technique is preferred from others techniques introduced in this work, because it is able to measure temperature for inhomogeneously seeded flow, and for its low facility set up compare to the dual-excitation wavelength technique.

Anisole mixed with isooctane is selected as fuel tracer, for its satisfactory physical and spectroscopy properties at 266 nm. Anisole absorption and fluorescence are studied for a pressure range of 0.2-4 MPa, a temperature range of 473-773 K, a constant concentration of  $1.29 \times 10^{12} \text{ molecule / cm}^3$ , a laser intensity of 90 mJ/pulse in different bath gases as nitrogen, carbon dioxide, argon and air.

Anisole presents a fluorescence emission band between 270-400 nm and the peak is located at 295 nm. For the studied temperatures, the fluorescence signal decreases with increasing pressure from 0.2 to 4 MPa. This decrease could be due to high collision rate leading to more non-radiative collisional desexcitation. Regarding the influence of temperature, the fluorescence quantum yield decreases significantly with increasing temperature for the studied pressure range. This important decrease is due to a vibrational energy increase, with more efficient radiative mechanisms of intersystem crossing.

From these experimental results, the temperature can be inferred from the fluorescence ratio for the excitation wavelength of 266 nm and the detection band. An optimised couple of detection band is found for  $\Delta\lambda_1 = 291\text{-}312 \text{ nm}$  and  $\Delta\lambda_2 = 374\text{-}395 \text{ nm}$ .

This combination corresponds to commercial band-pass filters called BrightLine FF01-292/27-50 and BrightLine FF01-386/23-50 (Semrock).

The comparison between the calculating and experimental fitting from the filtered gives a good agreement. Calibration curves are presented in a large

range of temperature, pressure and bath gases, in conditions close to those encountered in RCM. These calibrations are correct for the assumption where quasi-static results present a similar behaviour to dynamic measurements in RCM.

## Acknowledgements

This work was performed during the PhD thesis of K.H. Tran supported by the FUI (French Fond Unique Interministériel) in the framework of the MODELESSAIS Pôles de Compétitivité MOVE'O project.

## References

- [1] C. Schulz and V. Sick, Prog. Energy Combust. Sci. 31 (2005) 75.
- [2] M.C. Thurber and R.K. Hanson, Exp. Fluids 30 (2001) 93.
- [3] M. Luong, R. Zhang, C. Schulz and V. Sick, Appl. Phys. B 91 (2008) 669.
- [4] W. Koban, J.D. Koch, R.K. Hanson, C. Schulz, Phys. Chem. Chem. Phys. 6 (2004) 2940.
- [5] S. A. Kaiser and M. B. Long, Proc. Combust. Inst. 30 (2005) 1555.
- [6] M. Kühni, C. Morin, P. Guibert, Appl. Phys. B 102 (2011) 659.
- [7] M.Pasquini, N.Schiccheri, M.Becucci, G.Pietraperzia, Journal of Molecular Structure, 924-926 (2009), 457.
- [8] H. Hippler, J. Troe, and H.J. Wendelken, J.Chem. Phys. 78(11), (1983).
- [9] L.J.H. Hoffmann, S. Marquardt, A.S. Gemechu and H. Baumgärtel, Physical Chemistry Chemical Physics 8 (2006) 2360-237
- [10] R. Matsumoto, K. Sakeda, Y. Matsushita, T. Suzuki, Teijiro Ichimaru, Journal of Molecular Structure 735-736 (2006),153.
- [11] M. Takayanagi and I. Hanazaki, Laser Chem, 14 (1994) 103
- [12] M. Orain, P. Baranger, B. Rossow, F. Grisch, Appl. Phys. B 100 (2010) 945.
- [13] M. Orain, P. Baranger, B. Rossow, F. Grisch, Appl. Phys. B 102 (2011) 163.